

1 Size-resolved characteristics of inorganic ionic species in 2 atmospheric aerosols at a regional background site on the 3 South African Highveld

4
5 Andrew D. Venter¹, Pieter G. van Zyl^{1*}, Johan P. Beukes¹, Jan-Stefan Swartz¹, Miroslav Josipovic¹, Ville
6 Vakkari², Lauri Laakso^{1,2} and Markku Kulmala³

7
8 ¹Unit for Environmental Sciences and Management, North-West University, Potchefstroom, South Africa

9 ²Finnish Meteorological Institute, Helsinki, Finland

10 ³Department of Physics, University of Helsinki, Finland

11
12 Correspondence to: Pieter G. van Zyl, e-mail: pieter.vanzyl@nwu.ac.za, tel: +27 (0) 18 299 2353, fax: +27 (0)
13 18 299 2350.

15 Abstract

16 Aerosols consist of organic and inorganic species, and the composition and concentration of these species
17 depends on their sources, chemical transformation and sinks. In this study an assessment of major inorganic ions
18 determined in three aerosol particle size ranges collected for one year at Welgegund in South Africa was
19 conducted. SO_4^{2-} and ammonium (NH_4^+) dominated the PM_{10} size fraction, while SO_4^{2-} and nitrate (NO_3^-) dominated
20 the $\text{PM}_{1-2.5}$ and $\text{PM}_{2.5-10}$ size fractions. SO_4^{2-} had the highest contribution in the two smaller size fractions, while
21 NO_3^- had the highest contribution in the $\text{PM}_{2.5-10}$ size fraction. SO_4^{2-} and NO_3^- levels were attributed to the impacts
22 of aged air masses passing over major anthropogenic source regions. Comparison of inorganic ion concentrations
23 to levels thereof within a source region influencing Welgegund, indicated higher levels of most species within the
24 source region. However, the comparative ratio of SO_4^{2-} was significantly lower due to SO_4^{2-} being formed distant
25 from SO_2 emissions and submicron SO_4^{2-} having longer atmospheric residencies. The PM at Welgegund was
26 determined to be acidic, mainly due to high concentrations of SO_4^{2-} . PM_{10} and $\text{PM}_{1-2.5}$ fractions revealed a seasonal
27 pattern, with higher inorganic ion concentrations measured from May to September. Higher concentrations were
28 attributed to decreased wet removal, more pronounced inversion layers trapping pollutants, and increases in

1 household combustion and wild fires during winter. Back trajectory analysis also revealed higher concentrations
2 of inorganic ionic species corresponding to air mass movements over anthropogenic source regions.

3

4 **Keywords:** particulate matter; sulphate; nitrate; aerosol acidity; Welgegund

5

1 1 Introduction

2 Atmospheric aerosols or particulate matter (PM) are important components of the atmosphere with high
3 temporal and spatial variability, which can have significant impacts on air quality and climate change (Boucher et
4 al., 2013). Detailed physical and chemical characterisation are crucial in establishing the impacts of atmospheric
5 aerosols (e.g. Andreae and Rosenfeld, 2008; Brunekreef and Holgate, 2002; Pope and Dockery, 2006; Pöschl,
6 2005). PM is usually classified according to their size as coarse (PM_{10} – aerodynamic diameter $< 10 \mu\text{m}$), fine
7 ($PM_{2.5}$ – aerodynamic diameter $< 2.5 \mu\text{m}$), submicron (PM_1 – aerodynamic diameter $< 1 \mu\text{m}$) and ultrafine ($PM_{0.1}$
8 – aerodynamic diameter $< 0.1 \mu\text{m}$) particulates. PM consists of a large number of chemical species (e.g. Booyens
9 et al., 2015; Jimenez et al., 2009; Tiitta et al., 2014) of which the major inorganic ionic species usually considered
10 include sulphate (SO_4^{2-}), nitrate (NO_3^-) and ammonium (NH_4^+), sodium (Na^+), potassium (K^+), chloride (Cl^-),
11 calcium (Ca^{2+}), magnesium (Mg^{2+}) and fluoride (F^-).

12 South Africa is a well-known source region of atmospheric pollutants as indicated by ground measurements
13 and satellite retrievals over this region (e.g. Ghudea et al., 2009; Lourens et al., 2012; Sinha et al., 2004). South
14 Africa has the largest industrialised economy in Africa, with significant industrial, mining and agricultural
15 activities. Electricity is predominantly generated with coal-fired power plants that are centralised in the interior of
16 South Africa. In addition, seasonal biomass burning (wild fires) also has a large impact on this region (e.g. Vakkari
17 et al., 2013; 2014; Wai et al., 2014). In the interior of South Africa, the Welgegund measurement station (Beukes
18 et al., 2013) located 100 km west of Johannesburg enables representative sampling of aerosols from both industrial
19 source regions and regional background (Jaars et al., 2014; Tiitta et al., 2014), as well as studies on aerosol source
20 processes such as biomass burning and new particle formation (Vakkari et al., 2014, 2015).

21 In this study, an assessment of major inorganic ions determined in three aerosol size ranges (PM_1 , $PM_{1-2.5}$,
22 $PM_{2.5-10}$) collected for one year at Welgegund is presented. The measurement of inorganic ions is especially
23 important in South Africa, since the coal-fired power stations and most of the industries do not apply de-SO_x and
24 de-NO_x technologies, which leads to elevated emissions of sulphur dioxide (SO_2) and nitrogen dioxide (NO_2), and
25 the consequent formation of SO_4^{2-} and NO_3^- . This paper is an extension of work presented in two previous papers
26 wherein trace metals (Venter *et al.*, 2015) and organic compounds (Booyens *et al.*, 2014) determined in different
27 size ranges for atmospheric aerosols collected at Welgegund were presented. In addition, this work supplements
28 the work conducted by Tiitta *et al.* (2014), where PM_1 aerosols were chemically characterised with an aerosol
29 chemical specification monitor (ACSM) (Ng *et al.*, 2011) during which organic aerosol (OA), SO_4^{2-} , NH_4^+ , NO_3^-
30 and Cl^- concentrations were determined on-line with 30-minute time resolution. Furthermore, inorganic ion

1 concentrations determined at Welgegund (a regional background site) are compared with levels of these species
2 within a declared air quality priority area (indicating a source region with significantly high pollutant
3 concentrations), which is also one of the major anthropogenic source regions impacting on Welgegund. These
4 latter measurements were conducted at Marikana that is situated within the Bushveld Igneous Complex that forms
5 part of the Waterberg Priority Area (Government Gazette, 2012).

6 7 **2 Experimental**

8 **2.1 Site description**

9 2.1.1 Welgegund

10 Aerosol sampling was performed at the Welgegund atmospheric measurement station
11 (www.welgegund.org, 26.569786 S and 26.939289 E, 1 480 m a.s.l.). Welgegund is situated on a commercially
12 owned farm with no large pollution sources within proximity (~100 km). The site is situated in the interior of
13 South Africa so that it is frequently impacted by air masses moving over the most important source regions in the
14 interior of South Africa (e.g. the western Bushveld Igneous Complex, Vaal Triangle, Mpumalanga Highveld and
15 the Johannesburg-Pretoria conurbation), as well as a relatively clean background region with no large point
16 sources. In Beukes et al. (2013), Jaars et al. (2014) and Tiitta et al. (2014), maps indicating the location of
17 Welgegund and a detailed description of site, which include site selection, prevailing biomes and major source
18 regions are presented. Of the auxiliary measurements at Welgegund (Petäjä et al., 2013) only precipitation (by a
19 Vaisala QMR102 tipping bucket) are utilised in this study.

20 21 2.1.2 Marikana

22 Marikana (25.69845 S, 27.48056 E, 1170 m a.s.l.) is a village situated approximately 35 km east of
23 Rustenburg, 110km north of Welgegund. Maps indicating the location of Marikana were presented by Hirsikko et
24 al. (2012), Van Zyl et al. (2014) and Venter et al. (2012). Marikana is located within the western Bushveld Igneous
25 Complex, which is well known for comprehensive mining and metallurgical activities (Beukes et al., 2013; Van
26 Zyl et al., 2014; Venter et al., 2012). The site was situated in a residential area on the property of the Marikana
27 municipal clinic. A detailed description of the measurement site and possible sources of pollutants are presented
28 in Venter et al. (2012).

2.2 Sampling and analysis

PM samples were collected at Welgegund from 24 November 2010 until 28 December 2011. A Dekati (Dekati Ltd., Finland) PM₁₀ cascade impactor (ISO23210) equipped with Teflon filters was used to collect different particulate size ranges, i.e. PM_{2.5-10}, PM_{1-2.5} and PM₁. The pump flow rate was set at 30 L/min. Samples were collected continuously for one week, after which filters were changed. A total of 54 samples were collected for each of the three size ranges.

An Airmetrics MiniVol™ portable air sampler was used for aerosol sample collection at Marikana for one year from November 2008 until October 2009. Two MiniVol samplers were used simultaneously to collect PM₁₀ and PM_{2.5} samples (Airmetrics, 2011). A programmable timer controlled the pump in order to achieve sample collection of 12 hours per day for six days, beginning either at 06:00 for daytime data, or at 18:00 for night time data. Each sample contained PM collected for 72 hours. The actual sampling time and flow rate (5 L/min) were taken into consideration to determine the atmospheric concentrations of the species. All filter samples collected at Welgegund and Marikana were sealed-off in containers, which were stored in a freezer prior to analyses.

The filters were divided into two equal parts by a specially designed punching system, to be able to analyse both trace metals (Venter et al., 2015) and inorganic ions using a single set of samples. The inorganic ions in the aerosols collected on the Teflon filters were extracted with 5 mL deionised water (18.2 MΩ) in an ultrasonic bath for 30 minutes. Extracted aqueous samples were subsequently analysed with a Dionex ICS 3000 ion chromatograph (IC), with an IonPac AG18 (2 mm x 50 mm) guard and IonPac AS18 (2 mm x 50 mm) analytical column. The inorganic ionic species determined (with their detection limits indicated in brackets) included SO₄²⁻ (9.4 ppb), NH₄⁺ (4.0 ppb), NO₃⁻ (6.0 ppb), Na⁺ (5.8 ppb), K⁺ (4.4 ppb), Cl⁻ (4.8 ppb), Ca²⁺ (14.2 ppb), Mg²⁺ (20.5 ppb) and F⁻ (10.4 ppb) (F⁻ were not determined for samples collected at Marikana due to limitations of the analytical technique at the time when these samples were analysed).

2.3 Air mass history analysis

Individual 96-hour back trajectories arriving hourly with an arrival height of 100 m were calculated with HYSPLIT 4.820.19 (Draxler & Hess, 2004; Lourens et al., 2011; Venter et al., 2012) for the entire sampling period. An arrival height of 100 m was chosen since the orography in HYSPLIT is not very well defined with lower arrival heights resulting in increased error margins on individual trajectory calculations, which are estimated as 10-30 % of the distance travelled (Stohl et al., 2002).

1 3 Results

2 3.1 Size resolved inorganic ion concentrations

3 In Fig. 1, the concentrations of each of the inorganic ionic species determined in the three size ranges for
4 Welgegund samples are presented. SO_4^{2-} , NH_4^+ , K^+ and F^- concentrations were significantly higher in the PM_1 size
5 fraction, with concentrations of these species in the PM_1 size fraction approximately an order of magnitude higher
6 compared to the levels of these species in the $\text{PM}_{1-2.5}$ and $\text{PM}_{2.5-10}$ size fractions. Slightly higher levels of NO_3^- , Cl^-
7 and Mg^{2+} were measured in the $\text{PM}_{2.5-10}$ size fraction in relation to levels of these species in the other two size
8 fractions, while Na^+ and Ca^{2+} concentrations were evenly distributed in all three size ranges. SO_4^{2-} levels in PM_1
9 were approximately three times higher than NH_4^+ in the PM_1 size fraction, while being an order magnitude higher
10 compared to the concentrations of NO_3^- , Na^+ , K^+ and Ca^{2+} in all three size ranges, as well as to the concentrations
11 of SO_4^{2-} and NH_4^+ in the $\text{PM}_{1-2.5}$ and $\text{PM}_{2.5-10}$ size fractions. SO_4^{2-} concentrations in the PM_1 size fraction were two
12 orders of magnitude higher compared to Cl^- , Mg^{2+} and F^- levels in all three size ranges. The median SO_4^{2-} , NH_4^+ ,
13 K^+ and F^- concentrations in the PM_1 fraction were $1.35 \mu\text{g}/\text{m}^3$, $0.440 \mu\text{g}/\text{m}^3$, $0.032 \mu\text{g}/\text{m}^3$ and $0.015 \mu\text{g}/\text{m}^3$,
14 respectively. The median levels of NO_3^- , Cl^- and Mg^{2+} in the $\text{PM}_{2.5-10}$ size fraction were $0.057 \mu\text{g}/\text{m}^3$, $0.007 \mu\text{g}/\text{m}^3$
15 and $0.006 \mu\text{g}/\text{m}^3$, respectively. The highest median concentrations for Na^+ were $0.021 \mu\text{g}/\text{m}^3$ in the $\text{PM}_{1-2.5}$ size
16 fraction, while Ca^{2+} had the highest median of $0.014 \mu\text{g}/\text{m}^3$ in the $\text{PM}_{2.5-10}$ size fraction.

17

18 **Insert Fig. 1**

19

20 The normalised contribution percentages of each of the inorganic ionic species in terms of their ionic
21 concentrations observed at Welgegund are presented in Fig. 2 for the three size fractions. It is evident that the PM_1
22 size fraction is dominated by SO_4^{2-} and NH_4^+ , while the $\text{PM}_{1-2.5}$ and $\text{PM}_{2.5-10}$ size fractions are dominated by SO_4^{2-}
23 and NO_3^- . However, SO_4^{2-} was the most dominant species in both the smaller size fractions, while NO_3^- had the
24 highest concentration in $\text{PM}_{2.5-10}$. In South Africa SO_4^{2-} in the smaller size fractions (especially PM_1) can be
25 considered to be predominantly a secondary pollutant resulting from the oxidation of SO_2 in aged air masses (Tiitta
26 et al., 2014; Vakkari et al., 2015). Most industries in South Africa utilise particulate filters to filter out particulates
27 in off-gas. Therefore, primary emissions of SO_4^{2-} are unlikely. However, as mentioned previously, most industries
28 in South Africa do not employ de- SO_x and de- NO_x technologies (e.g. Collett et al., 2010; Lourens et al., 2011),
29 which leads to higher SO_2 and NO_2 emissions. Furthermore, the highly industrialised interior of South Africa is
30 characterised by anti-cyclonic recirculation of air masses wherein the aging of pollutant species occurs (Lourens

1 et al., 2012). Recently Vakkari et al. (2015) also indicated significant SO_4^{2-} formation in connection to new particle
2 formation in South Africa. Particulate NH_4^+ is almost exclusively a secondary formed aerosol (Seinfeld & Pandis
3 2006) and thus most of the inorganic ions in the PM_1 fraction at Welgegund can be considered to be of secondary
4 origin. As mentioned previously, Tiitta et al. (2014) chemically characterised PM_1 aerosols with an ACSM at
5 Welgegund, which also indicated higher contributions of SO_4^{2-} and NH_4^+ to the chemical content in PM_1 aerosols.

6
7 **Insert Fig. 2**

8
9 Atmospheric NO_3^- can mainly be attributed to the oxidation of NO_2 gaseous emissions associated
10 predominantly with fossil fuel combustion (e.g. coal-fired power stations) and industries not employing de- NO_x
11 technologies as mentioned above. Vehicular emissions also contribute to increased NO_2 emissions on the South
12 African Highveld (Lourens et al., 2016), while the significant contribution of household combustion for space
13 heating and cooking on NO_2 levels has also been indicated (e.g. Venter et al., 2012). The much lower NO_3^-
14 concentrations in the PM_1 fraction can be ascribed to the high SO_4^{2-} levels substituting NO_3^- in NH_4NO_3 (Seinfeld
15 & Pandis, 2006). In addition, the higher NO_3^- contribution in the $\text{PM}_{2.5-10}$ size fraction are indicative of the
16 influence of aged marine air masses, where hydrogen chloride has been displaced from NaCl by HNO_3 vapour to
17 form NaNO_3 (Turner & Colbeck, 2008). This is also signified by the higher percentage contribution of Na^+ in the
18 $\text{PM}_{2.5-10}$ size fractions. It is also important to note that since the primary sources of SO_2 and NO_2 in the northern
19 interior of South Africa are coal-fired power stations, SO_2 emissions are directly proportional to the amount of
20 coal combusted whereas NO_2 emissions vary depending on the burner technology implemented by each power
21 station (Pretorius et al., 2015). Therefore the relative SO_4^{2-} and NO_3^- concentrations could also be related to the
22 differences in emissions of SO_2 and NO_2 from coal-fired power plants.

23 Furthermore, the $\text{PM}_{2.5-10}$ size fraction also has higher percentage contributions from Cl^- , Mg^{2+} , Ca^{2+} and
24 Na^+ compared to the other two size fractions, which can be attributed to larger particles originating from marine
25 (e.g. Na^+ and Cl^-) and terrigenous sources (e.g. Ca^{2+} from wind-blown dust). Although Fig. 1 indicated that the
26 concentrations of Na^+ and Ca^{2+} species were evenly distributed in all three size fractions, much lower contributions
27 from SO_4^{2-} and NH_4^+ in the $\text{PM}_{2.5-10}$ size fraction lead to an increase in the relative contribution of these species to
28 the total inorganic ionic content. In addition, the NO_3^- , Cl^- and Mg^{2+} concentrations are higher in the $\text{PM}_{2.5-10}$ size
29 fraction (Fig. 1). The marine influence on the PM composition was also estimated by comparing the ratios of SO_4^{2-}
30 , Cl^- , Mg^{2+} , K^+ and Ca^{2+} to Na^+ (assuming Na^+ is only of marine origin) with reference ratios of these species with

1 regard to Na^+ as presented by Keene et al. (1986), which are presented in Table 1. The significantly higher ratios
2 of $\text{SO}_4^{2-}/\text{Na}^+$, K^+/Na^+ and $\text{Ca}^{2+}/\text{Na}^+$ compared to reference ratios indicate a very small contribution from marine
3 sources on levels of these species measured at Welgegund. However, the $\text{Mg}^{2+}/\text{Na}^+$ ratio in all three size fractions
4 were close to the sea water ratio, especially in the PM_1 size fraction, indicating a strong marine influence on Mg^{2+}
5 concentrations. The lower Cl^-/Na^+ ratio determined can be attributed to Cl^- depletion in marine air masses (Feng
6 et al., 2017) and the influence of non-marine species in the PM collected (Mouli et al., 2003).

7
8 **Insert Table 1**

9 10 **3.2 Acidity**

11 The acidity of atmospheric aerosols has an influence on their hygroscopicity, as well as their ability to
12 produce heterogeneous sulphate and secondary organic aerosols (Jang et al., 2002; Pathak et al., 2011). As
13 discussed by Tiitta et al. (2014), it is possible to estimate the acidity of PM by comparing the measured NH_4^+ mass
14 concentration to the amount of NH_4^+ needed to completely neutralise the anions that were calculated using Eq. (1):

$$16 \quad \text{NH}_4^+_{cal} = 18 \times \left(2 \times \frac{\text{SO}_4^{2-}}{96} + \frac{\text{NO}_3^-}{62} + \frac{\text{Cl}^-}{35.5} \right) \quad (1)$$

17
18 Here, SO_4^{2-} , NO_3^- and Cl^- are the mass concentrations of the ions ($\mu\text{g}/\text{m}^3$) and the denominators correspond to
19 their molecular weights, with 18 being the molecular weight of NH_4^+ . If the measured NH_4^+ concentration is lower
20 than the calculated values, particles are considered to be 'more acidic' or, if the two values are equal, they are
21 considered 'bulk neutralised'. This approach assumes a minimal influence of metal ions, organic acids and bases
22 on NH_4 concentration (Zhang et al., 2007). Only PM_1 was considered due to its significance in secondary aerosol
23 formation, while SO_4^{2-} and NH_4^+ were predominantly in the PM_1 size fraction as indicated in Fig. 2. The calculated
24 NH_4^+ concentrations plotted against the measured values for PM_1 are presented in Fig. 3. In this figure, the 1:1 line
25 corresponds to the bulk neutralised state, the dry months comprise the three driest months during the sampling
26 period, i.e. July 2011 to September 2011, and the wet months include the months with the highest rainfall, i.e.
27 December 2010 to February 2011 and November 2011 to December 2011. It is evident from the results that the
28 submicron aerosols are closer to the neutralised state in the dry months than in the wet months. However, during
29 wet and dry months, the PM_1 aerosols are essentially acidic in nature, implying that the atmospheric NH_4

1 concentration was insufficient to neutralise all SO_4^{2-} , NO_3^- and Cl^- anions. From the results presented in Fig. 1
2 and 2, it could be deduced that SO_4^{2-} was the dominating acidic ion, which indicates that a fraction of NO_3^- and
3 Cl^- anions must be associated with cations other than NH_4^+ . These results agree with previous observations by
4 Tiitta et al. (2014) obtained from PM_{10} measurements with an ACMS. In addition, Conradie et al. (2016) also
5 indicated that rain samples collected at four sites in the interior of South Africa were in most instances acidic, with
6 SO_4^{2-} also the main acidic ion. In Fig. 3, the circled points indicate values that did not lie close to the linear fitted
7 lines of the dry and wet season data. Although these data points were considered in the afore-mentioned linear fits,
8 they clearly indicate somewhat different behaviour. Obviously, these ‘outliers’ could be as a result of sampling
9 artefacts or the assumptions made in this approach, i.e. minimal influence of metal ions, as well as organic acids
10 and bases on NH_4 concentrations (Zhang et al., 2007). However, these data points could also indicate that the
11 aerosol acidities might be extremely acidic or basic on certain occasions, especially, aerosols in the wet season.
12 SO_4^{2-} levels in the wet season could also be possibly increased during cloud processing, which is considered to be
13 efficient in secondary SO_4^{2-} formation (Husain et al., 1991). Back trajectory analysis performed for these weeks
14 during which these outlier values were determined did not reveal any particular sources/source regions. It is
15 recommended that future studies utilise high-volume samplers to collect aerosol samples over shorter periods (e.g.
16 24 hours) to better quantify the influence of specific sources/source regions on the acidity of aerosols.

17

18 **Insert Fig. 3**

19

20 **3.3 Comparison with inorganic ion concentrations measured within a source region**

21 In order to contextualise the inorganic ion concentrations measured at Welgegund, the results were
22 compared to levels determined for inorganic ionic species at Marikana. As mentioned previously, Marikana is
23 situated within the industrialised Bushveld Igneous Complex, which is one of the major source regions influencing
24 air masses measured at Welgegund (Beukes et al., 2013; Jaars et al., 2014; Tiitta et al., 2014). Venter et al. (2012)
25 reported high PM_{10} concentrations measured at Marikana, with PM_{10} levels exceeding South African legislative
26 standard limits.

27 In Fig. 4, the concentrations of each of the inorganic ionic species determined in two size ranges, i.e. $\text{PM}_{2.5}$
28 and $\text{PM}_{2.5-10}$ at Marikana are presented. As mentioned, MiniVol samplers were used to collect total PM_{10} and $\text{PM}_{2.5}$
29 at Marikana. Therefore, $\text{PM}_{2.5-10}$ concentrations were calculated by subtracting $\text{PM}_{2.5}$ from the PM_{10} measurements.
30 Similar to measurements at Welgegund, SO_4^{2-} and NH_4^+ occurred predominantly in the smaller size fraction

1 (PM_{2.5}) with median concentrations of 1.83 µg/m³ and 0.55 µg/m³, respectively. K⁺ concentrations were also higher
2 in the PM_{2.5} size fraction with a median concentration of 0.09 µg/m³, while slightly higher median concentrations,
3 i.e. 0.09 µg/m³ and 0.07 µg/m³ were measured for Na⁺ and Cl⁻, respectively, in the PM_{2.5} size fraction compared
4 to the PM_{2.5-10} size fraction. Comparison of the concentrations of K⁺ in the different size fractions indicate a larger
5 concentration of K⁺ in the PM_{2.5-10} size fraction in relation to the PM_{2.5} size fraction at Marikana compared to
6 significantly lower concentrations measured at Welgegund in the PM_{2.5-10} size fraction with respect to the PM₁ and
7 PM_{1-2.5} size fractions. Na⁺ and Cl⁻ concentrations in the PM_{2.5-10} size fraction relative to the smaller size fractions
8 at Welgegund were also higher compared to PM_{2.5-10} levels in relation to PM_{2.5} concentrations measured at
9 Marikana. However, this can be attributed to the PM_{2.5} size fraction containing both the PM₁ and PM_{1-2.5} size
10 fractions. Ca⁺ and Mg⁺ concentrations were higher in the PM_{2.5-10} size fraction with median concentrations of 0.16
11 µg/m³ and 0.05 µg/m³, respectively, while the median NO₃⁻ concentration was marginally higher in the PM_{2.5-10}
12 size fraction, i.e. 0.28 µg/m³. The higher Ca⁺, Mg⁺ and NO₃⁻ concentrations determined in the PM_{2.5-10} size fraction
13 in relation to the PM_{2.5} size fractions are similar to the measurements at Welgegund where levels of these species
14 were also higher in the PM_{2.5-10} size fraction with respect to the smaller size fractions. At Marikana SO₄²⁻ levels
15 were approximately three and six times higher than NH₄⁺ and NO₃⁻ levels, respectively, while being an order
16 magnitude higher compared to the concentrations of Na⁺, K⁺, Ca²⁺, Cl⁻ and Mg²⁺ in both size ranges.

17

18 **Insert Fig. 4**

19

20 In Fig. 5, the normalised distribution percentages of the median concentrations of each inorganic ionic
21 species in the PM_{2.5} and PM_{2.5-10} size-fractions measured at Marikana are presented. It is evident that the PM_{2.5}
22 size fraction is dominated by SO₄²⁻, with NH₄⁺ being the second most abundant species, which is similar to
23 Welgegund where SO₄²⁻ and NH₄⁺ dominated the PM₁ and PM_{1-2.5} size fractions. The high SO₄²⁻ contributions in
24 the PM_{2.5} size fraction can be attributed to the strong influence of pyrometallurgical activities on the aerosols
25 sampled in this region. It is well known that the platinum group metals (PGM) industries in the western Bushveld
26 Igneous Complex are associated with high SO₂ emissions associated with sulphidic ores, without the concomitant
27 formation of NO₂ associated with coal-fired power plant emissions (Xiao and Laplante, 2004). Van Zyl et al.
28 (2014) also indicated the high elemental sulphur content in PM sampled in this region (as indicated with scanning
29 electron microscopy-energy dispersive spectrometry). In addition, the highest contribution of NO₃⁻ in the PM_{2.5-10}

1 size fractions at Marikana is similar to Welgegund where NO_3^- also had the highest concentration in the $\text{PM}_{2.5-10}$
2 size fraction. The contribution of Ca^{2+} in the $\text{PM}_{2.5-10}$ size fraction at Marikana, which is the second most abundant
3 species in this size fraction at Marikana, is also similar to the contribution of Ca^{2+} at Welgegund. However, a larger
4 contribution of Na^+ in the $\text{PM}_{2.5-10}$ size fraction is observed at Welgegund compared to Marikana.

5
6 **Insert Fig. 5**

7
8 In general, the concentrations of all the inorganic species were higher at Marikana compared to Welgegund,
9 with the exception of NH_4^+ that had similar concentrations in the PM_1 and $\text{PM}_{2.5}$ size fractions at Welgegund and
10 Marikana, respectively. SO_4^{2-} levels in the smaller size fractions (PM_1 and $\text{PM}_{2.5}$ size fractions at Welgegund and
11 Marikana, respectively) were approximately 1.5 times higher at Marikana, while concentrations of NO_3^- , Cl^- , Mg^{2+}
12 Na^+ and Ca^{2+} were an order of magnitude higher compared to levels thereof at Welgegund in the PM_1 , $\text{PM}_{2.5}$ and
13 $\text{PM}_{2.5-10}$ size fractions. K^+ levels in the $\text{PM}_{2.5}$ size fraction at Marikana (the smallest size fraction measured at
14 Marikana that also contains PM_1 aerosols) were approximately 3 times higher than K^+ concentrations at
15 Welgegund in the PM_1 size fraction (the size fraction that contained the highest K^+ concentration). Higher levels
16 of inorganic species are expected, since Marikana is situated within a source region with a large number of
17 industrial and mining activities, as well as a dense population that contributes to emissions from household
18 combustion for space heating and cooking. However, it is of significance to note that, although SO_4^{2-} levels were
19 higher at Marikana compared to the regional background Welgegund site, the ratio (approximately 1.5) was
20 substantially lower compared to the comparative ratios of other inorganic species measured at Marikana and
21 Welgegund. This observation signifies the regional, and not only local, impact of SO_2 emissions from
22 pyrometallurgical industries in the western Bushveld Igneous Complex. As mentioned previously, SO_4^{2-} is
23 predominantly a secondary pollutant in South Africa, which can be formed distant from SO_2 sources. Therefore,
24 SO_4^{2-} levels can also be relatively high at sites considered to be regional background or remote sites. SO_4^{2-} levels
25 at the industrialised Marikana site can also be additionally influenced by the regional impact of SO_2 emissions
26 from coal-fired power stations. In addition, SO_4^{2-} occurs predominantly in submicron particles that have longer
27 atmospheric lifetimes and are transported over longer distances, compared to e.g. NO_3^- in larger particles that are
28 deposited faster from the atmosphere and closer to the source. This is also substantiated by similar concentrations
29 determined for NH_4^+ at Marikana and Welgegund. Conradie et al. (2016) also indicated that SO_4^{2-} were the
30 dominant inorganic ion in rain samples collected, not only within proximity of anthropogenic sources, but also at

1 remote and/or background sites in the north-eastern interior of South Africa. The regional impacts of SO_4^{2-} have
2 also been indicated for other areas in the world (e.g. Yeh et al., 2015). Laban et al. (2018) also showed that
3 concentrations of the secondary pollutant, O_3 , were high at sites in the north-eastern interior of South Africa
4 considered to be background sites due the regional impacts of precursor species.

5 As mentioned previously, day- and night-time samples were collected at Marikana. Comparisons between
6 the concentrations of the inorganic ions measured during day- and night-time in the PM_{10} and $\text{PM}_{2.5}$ size fractions
7 did not reveal significant differences in concentrations of the ionic species, with the exception of NO_3^- and Cl^-
8 concentrations in the $\text{PM}_{2.5}$ size fraction that were higher during night time, as indicated in Fig. 6. Venter et al.
9 (2012) indicated increased NO_2 concentrations during night-time associated with household combustion at
10 Marikana, which can be related to increased night-time NO_3^- . Cl^- can be associated with fresh biomass burning
11 emissions (Aurela et al., 2016) and therefore higher night-time Cl^- can also be attributed to the influence of
12 household combustion.

13
14 **Insert Fig. 6**

16 **3.4 Temporal and spatial variability**

17 In Fig. 7, the total monthly concentrations of the inorganic ionic species in $\text{PM}_{2.5-10}$ (a), $\text{PM}_{1-2.5}$ (b) and PM_1
18 (c) measured at Welgegend are presented, with the contributing concentrations of each of the inorganic ions
19 indicated. No distinct seasonal pattern is observed for the $\text{PM}_{2.5-10}$ size fraction. However, the $\text{PM}_{1-2.5}$ and PM_1 size
20 fractions indicated higher inorganic ion concentrations from May to September and May to August, respectively.
21 These periods with elevated inorganic ion levels can at least partially be ascribed to seasonal variations in
22 meteorological parameters. The months with higher inorganic ion concentrations in the $\text{PM}_{1-2.5}$ and PM_1 size
23 fractions coincide with the cold and dry winter months experienced in this part of South Africa. Winter in South
24 Africa occurs typically between June and August, which is associated with increased air mass recirculation, as
25 well as more pronounced lower inversion layers that inhibit vertical mixing in the atmosphere and trap pollutant
26 species near the surface (Grstang, 1996). Winter is also related to additional combustion of coal and wood for
27 domestic heating, which results in elevated aerosol particle concentrations (Vakkari et al., 2013; Venter et al.,
28 2012). Furthermore, this part of South Africa is characterised by distinct wet and dry seasons, with the dry season
29 occurring typically between mid-May and mid-October (Tiitta et al., 2014). In Fig. 8, the monthly precipitation
30 measured during the entire sampling period at Welgegend is presented, which clearly indicates a period with low

1 rainfall, i.e. May to September. Therefore, the removal rate of atmospheric PM is also reduced during these dry
2 months. The influence of wet deposition on atmospheric inorganic ion concentrations is also illustrated by the
3 difference in the concentrations measured for December 2010 and December 2011 (Fig. 7). Precipitation was
4 higher in December 2010 compared to December 2011, which resulted in increased wet deposition of inorganic
5 ionic species in December 2010. In addition, the periods with elevated levels of inorganic ions in the PM_{1-2.5} and
6 PM₁ size fractions coincide with increased occurrences of biomass burning (wild fires) from July to September
7 (e.g. Vakkari et al., 2013 and 2014). Furthermore, although no clear seasonal pattern is observed for PM_{2.5-10}, the
8 influence of weather (winter and precipitation) is to a certain extent reflected in higher inorganic ion concentrations
9 measured in July and September in this size fraction, as well as much lower inorganic ion concentrations measured
10 in December 2010 and January 2011, i.e. months associated with higher rainfall. (Fig. 8).

11

12 **Insert Fig. 7**

13 **Insert Fig. 8**

14

15 ACSM measurements conducted by Tiitta et al. (2014) indicated that SO₄²⁻, NH₄⁺, NO₃⁻ and Cl⁻
16 concentrations in PM₁ depended strongly on air mass history. Therefore, back trajectory analysis were performed
17 for each of the sampling months, which are presented in Fig. 9 in order to establish the influence of air mass history
18 on monthly inorganic ion concentrations. In Fig. 9, the typical source areas are represented by polygons. The blue
19 polygon indicates the combined Vaal Triangle Airshed Priority Area, Highveld Priority Area and Gauteng (i.e.
20 Johannesburg-Pretoria megacity conurbation). The red polygon incorporates the Waterberg Priority Area and the
21 typical anti-cyclonic recirculation pathway of air masses sampled at Welgegund. From Fig. 9, it is evident that the
22 frequency of air masses arriving at Welgegund passing over the two source regions and the background regions is
23 different for certain months.

24

25 **Insert Fig. 9**

26

27 Similar air mass movements are observed for December 2010, April 2011, May 2011, August 2011,
28 October 2011, November 2011 and December 2011 indicating frequent influences from the anti-cyclonic
29 recirculation pathway passing over the Bushveld Igneous Complex (part of the Waterberg Priority Area)
30 (Government Gazette, 2012). The difference in inorganic ion concentrations measured in December 2010 and

1 December 2011 can be ascribed to the influence of wet deposition on atmospheric PM, as discussed previously
2 (Fig. 8). The inorganic ion levels determined in April 2011, October 2011, November 2011 and December 2011
3 were similar in all three size fractions, with the exception of inorganic ion concentrations in PM_{1-2.5} in October.
4 These months also had similar levels of rainfall, as indicated in Fig. 8. Higher inorganic ion concentrations were
5 determined in May 2011 and August 2011 (especially in May 2011) in the PM₁ and PM_{1-2.5}, which can be attributed
6 to these months being dry leading to a decrease in wet removal thereof. During June 2011, much lower inorganic
7 ion concentrations were determined in the PM₁ and PM_{1-2.5} size fractions compared to the higher inorganic ion
8 concentrations measured in these two size fraction during the other colder and dryer months (May to September).
9 Back trajectory analysis (Fig. 9) reveals that during June 2011, Welgegund was much more frequently impacted
10 by air masses passing over the background region, leading to lower concentrations of inorganic ions. It is also
11 evident from Fig. 9 that Welgegund was more frequently influenced by air masses passing over the Johannesburg-
12 Pretoria conurbation in July 2011, with associated higher inorganic ion concentrations in all three size fractions,
13 especially in the PM_{2.5-10} size fractions. January 2011 and February 2011 back trajectories indicated more frequent
14 influences from marine air masses at Welgegund, which are reflected in the higher NO₃⁻ and Na⁺ concentrations
15 measured in the PM_{2.5-10} size fraction in February 2011. As mentioned previously, the lower inorganic ion
16 concentrations in January 2011 can be attributed to high precipitation and the associated wet deposition (Fig. 8).

17 The monthly concentrations of each of the inorganic ions in the three size fractions reflect the normalised
18 contributing concentrations for the entire sampling period at Welgegund presented in Fig. 2, i.e. the smaller size
19 fractions are dominated by SO₄²⁻, while NO₃⁻ concentrations were the highest in the PM_{2.5-10} size fractions. The
20 relatively large contribution from NH₄⁺ in the PM₁ size fraction is also evident for each of the months, while the
21 influence of the marine and crustal species on the PM_{2.5-10} size fraction is also reflected in the monthly
22 concentrations. A distinct seasonal pattern is observed for NO₃⁻ in the PM₁ size fraction, with NO₃⁻ concentrations
23 only evident from June to October with elevated concentrations thereof from July to September. These higher NO₃⁻
24 levels coincide with the peak biomass burning season from July to September. Vakkari et al. (2014) indicated that
25 aerosols in fresh biomass burning (wild fires) plumes measured at Welgegund consisted of 7 to 10% NO₃⁻. In aged
26 biomass burning plumes, lower NO₃⁻ concentrations are expected, since SO₄²⁻ would have reacted with NH₄NO₃,
27 which effectively removes NO₃⁻ from that particulate phase. Therefore, fresh biomass burning plumes can be
28 considered a source of NO₃⁻ in the PM₁ size fraction. Higher NO₃⁻ concentrations are also evident in August and
29 September in the PM_{1-2.5} size fractions, which can also be attributed to biomass burning emissions. A similar
30 seasonal pattern is observed for Cl⁻ in the PM_{1-2.5} size fraction with relatively higher Cl⁻ levels from July to

1 September, which can be attributed to primary biomass burning emissions (Vakkari et al., 2014). Tiitta et al. (2014)
2 indicated a strong influence of biomass burning on organic aerosol and total PM₁ concentrations. In addition,
3 Aurela et al. (2016) indicated that KCl was likely to occur in fresh smoke of burning savannah grass. However, a
4 less significant impact of biomass burning is observed on the inorganic ionic species concentrations.

5

6 **4 Conclusions**

7 This paper presents the concentrations of inorganic ion species determined in aerosol samples collected in
8 three size ranges, i.e. PM₁, PM_{1-2.5} and PM_{2.5-10} collected at Welgegund. SO₄²⁻ concentrations in the PM₁ size
9 fraction were significantly higher compared to the other species in all three size fractions, as well as levels thereof
10 in the PM_{1-2.5} and PM_{2.5-10} size ranges. NH₄⁺ in the PM₁ size fraction and NO₃⁻ in the PM_{2.5-10} size fraction were
11 the second and third most abundant species, respectively. Normalised contribution percentages indicated that SO₄²⁻
12 and NH₄⁺ dominated the PM₁ size fraction, while SO₄²⁻ and NO₃⁻ were the predominant species in the PM_{1-2.5} and
13 PM_{2.5-10} size fractions. SO₄²⁻ had the highest contribution in the two smaller size fractions, while NO₃⁻ had the
14 highest contribution in the PM_{2.5-10} size fraction. SO₄²⁻ and NO₃⁻ levels were attributed to the impacts of aged air
15 masses passing over source regions with high SO₂ and NO₂ emissions, while marine air masses were also
16 considered a source of NO₃⁻.

17 In general it is concluded that the anthropogenic SO₄²⁻ dominates the inorganic ion budget at Welgegund
18 and causes the aerosol to be acidic, which may have adverse implications for the environment (Jang et al., 2002;
19 Pathak et al., 2011).

20 Comparison of the inorganic ion concentrations measured at Welgegund to measurements of these species
21 at Marikana, which is situated within one of the major anthropogenic/industrial source regions influencing
22 Welgegund, indicated that the concentrations of almost all the inorganic ion species were higher at Marikana.
23 SO₄²⁻ concentrations were also the highest at Marikana, which were approximately 1.5 times higher compared to
24 levels thereof Welgegund. The concentrations of most of the other species were an order of magnitude higher. The
25 smaller size fraction at Marikana was also dominated by SO₄²⁻ and NH₄, while the larger size fraction was also
26 dominated by NO₃⁻. The comparative ratio of SO₄²⁻ at Marikana and Welgegund was significantly lower in relation
27 to the comparative ratios of most of the other inorganic ions at the two sites, which was attributed to the SO₄²⁻
28 being a secondary aerosol that can be formed distant from the sources of SO₂, as well as SO₄²⁻ occurring
29 predominantly in submicron particulates that can be transported over longer distances in the atmosphere and
30 influence background/remote sites.

1 The PM₁ and PM_{1-2.5} fractions indicated higher inorganic ion concentrations from May to September. These
2 months coincide with the colder and dryer months in this part of South Africa. Therefore, higher concentrations
3 were mainly attributed to increases in pollutant concentrations associated with recirculation of air masses, more
4 pronounced inversion layers trapping pollutants near the surface and increased emissions, in conjunction with a
5 decrease in the wet removal of these species. In addition, air mass history of each of the sampling months revealed
6 higher concentrations of inorganic ionic species corresponding to air mass movements over source regions, which
7 also emphasises the significance of anthropogenic sources at Welgegund. Furthermore, biomass burning, which
8 significantly affects OA (Tiitta et al., 2014), has only a minor effect (~10%) on inorganic ion concentrations by
9 being a source of NO₃, Cl (and possibly K in PM₁) as indicated by increases in these species during the biomass
10 burning season.

11

12 **5 Acknowledgements**

13 The financial assistance of the National Research Foundation (NRF) towards this research is hereby
14 acknowledged. Opinions expressed and conclusions arrived at are those of the authors and are not necessarily to
15 be attributed to the NRF. The authors would also like to acknowledge financial support by the Academy of Finland
16 Center of Excellence program (grant no. 272041).

17

18 **6 References**

- 19 Airmetrics. MiniVol portable air sampler. Operation manual version 4.2c. Eugene, OR 97403, USA (2011)
- 20 Andreae, M.O., Rosenfeld, D.: Aerosol – cloud – precipitation interactions. Part 1. The nature and sources of
21 cloud-active aerosols. *Earth Sci Rev.* 89, 13–41 (2008) doi:10.1016/j.earscirev.2008.03.001
- 22 Aurela, M., Beukes, J.P., Van Zyl, P.G., Vakkari, V., Teinilä, K., Saarikoski, S., Laakso, L.: The composition of
23 ambient and fresh biomass burning aerosols at a savannah site, South Africa. *S. Afr. J. Sci.* 112(5/6), Art.
24 #2015-0223, 8 pages. (2016) <http://dx.doi.org/10.17159/sajs.2016/20150223>
- 25 Beukes, J.P., Vakkari, V., Van Zyl, P.G., Venter, A.D., Josipovic, M., Jaars, K., Tiitta, P., Kulmala, M., Worsnop,
26 D., Pienaar, J.J., Järvinen, E., Chellapermal, R., Ignatius, K., Maalick, Z., Cesnulyte, V., Ripamonti, G.,
27 Laban, T.L., Skrabalova, L., Du Toit, M., Virkkula, A., Laakso, L.: Source region plume characterisation
28 of the interior of South Africa, as measured at Welgegund. *Clean air journal.* 23(1), 1-10 (2013)
- 29 Beukes, J.P., Venter, A.D., Josipovic, M., **Van Zyl, P.G.**, Vakkari, V., Jaars, K., Dunn, M. and Laalso, L., Chapter
30 6: Automated continuous air monitoring, In: Forbes, P., Editor, *Monitoring of air pollutants: Sampling,*

1 sample, preparation and analytical techniques, Volume 70, pp. 183–208, Elsevier, Amsterdam (2015) doi:
2 10.1016/bs.coac.2015.09.006

3 Booyens, W., Van Zyl, P.G., Beukes, J.P., Ruiz-Jimenez, J., Kooperi, M., Riekkola, M.-L., Josipovic, M., Venter,
4 A.D., Jaars, K., Laakso, L., Vakkari, V., Kulmala, M., Pienaar, J.J.: Size-resolved characterisation of
5 organic compounds in atmospheric aerosols collected at Welgegund, South Africa. *J. Atmos. Chem.* 72,
6 43–64 (2015) doi:10.1007/s10874-015-9304-6

7 Boucher, O., Randall, D., Artaxo, P., Bretherton, C., Feingold, G., Forster, P., Kerminen, V.-M., Kondo, Y., Liao,
8 H., Lohmann, U., Rasch, P., Satheesh, S.K., Sherwood, S., Stevens, B., Zhang, X.Y.: Clouds and Aerosols.
9 Climate Change: The Physical Science Basis. Contribution of Working Group I to the Fifth Assessment
10 Report of the Intergovernmental Panel on Climate Change [Stocker, T.F., D. Qin, G.-K. Plattner, M. Tignor,
11 S.K. Allen, J. Boschung, A. Nauels, Y. Xia, V. Bex and P.M. Midgley (eds.)]. Cambridge University Press,
12 Cambridge, United Kingdom and New York, NY, USA (2013)

13 Brunekreef, B., Holgate, S.T: Air pollution and health. *Lancet.* 360(9341), 1233-1242 (2002)
14 [http://dx.doi.org/10.1016/S0140-6736\(02\)11274-8](http://dx.doi.org/10.1016/S0140-6736(02)11274-8)

15 Conradie, E.H., Van Zyl, P.G., Pienaar, J.J., Beukes, J.P., Galy-Lacaux, C., Venter, A.D., Mkhathshwa, G.V.: The
16 chemical composition and fluxes of atmospheric wet deposition at four sites in South Africa. *Atmos.*
17 *Environ.* 146, 113-131 (2016) <http://dx.doi.org/10.1016/j.atmosenv.2016.07.033>

18 Draxler, R. R. and Hess, G. D. Description of the HYSPLIT 4 Modelling System. NOAA Technical Memorandum,
19 ERL ARL-224 (2004)

20 Feng, L, Shen, H, Zhu, Y, Gao, H, Yao, X,;Insight into Generation and Evolution of Sea-Salt Aerosols from Field
21 Measurements in Diversified Marine and Coastal Atmospheres. *Scientific Reports* 7, 41260 (2017) doi:
22 10.1038/srep41260

23 Garstang, M., Tyson, P.D., Swap, R., Edwards, M., Kallberg, P., Lindesay, J.A: Horizontal and vertical transport
24 of air over southern Africa. *J. Geophys. Res.* 101(D19), 23721–23736 (1996) doi:10.1029/95JD00844

25 Ghudea, S.D., Van Der A, R.J., Beiga, G., Fadnavis, S., Poladea, S.D.: Satellite derived trends in NO₂ over the
26 major global hotspot regions during the past decade and their inter-comparison. *Environ. Pollut.*
27 157(6),1873-1878 (2009) doi:10.1016/j.envpol.2009.01.013

28 Government Gazette. 2012. Notice 495 of 2012. Department of Home Affairs, National Environmental
29 Management: Air Quality Act, 2004, Declaration of the Waterberg National Priority Area, South African

1 Government Gazette No. 35345 on 15 June 2012; Correction notice (154): Waterberg-Bojanala National
2 Priority Area, South African Government Gazette No. 36207 on 8 March 2013

3 Held, G., Gore, B.J., Surridge, A.D., Tosen, G.R., Turner, C.R., Walmsley, R.D.: Air pollution and its impacts on
4 the South African Highveld. Environmental Scientific Association, Cleveland, pp. 128 (1996)

5 Hirsikko, A., Vakkari, V., Tiitta, P., Manninen, H. E., Gagné, S., Laakso, H., Kulmala, M., Mirme, A., Mirme, S.,
6 Mabaso, D., Beukes, J. P., Laakso, L.: Characterisation of sub-micron particle number concentrations and
7 formation events in the western Bushveld Igneous Complex, South Africa. *Atmos. Chem. Phys.* 12, 3951–
8 3967 (2012) doi:10.5194/acp-12-3951-2012

9 Husain, L., Dutkiewicz, V. A., Hussain, M. M., Khwaja, H. A., Burkhard, E. G., Mehmood, G., Parekh, P. P.,
10 Canelli, E.: A study of heterogeneous oxidation of SO₂ in summer clouds. *J. Geophys. Res.*, 96(D10),
11 18789–18805 (1991) doi:10.1029/91JD01943

12 Jaars, K., Beukes, J.P., Van Zyl, P.G., Venter, A.D., Josipovic, M., Pienaar, J.J., Vakkari, V., Aaltonen, H., Laakso,
13 H., Kulmala, M., Tiitta, P., Guenther, A., Hellén, H., Laakso L., Hakola, H.: Ambient aromatic hydrocarbon
14 measurements at Welgegund, South Africa. *Atmos. Chem. Phys.* 14, 7075–7089 (2014) doi:10.5194/acp-
15 14-7075-2014

16 Jang, M. S., Czoschke, N. M., Lee, S., Kamens, R. M.: Heterogeneous atmospheric aerosol production by acid-
17 catalyzed particle-phase reactions. *Science*, 298, 814–817 (2002) doi:10.1126/science.1075798

18 Jimenez, J.L., Canagaratna, M.R., Donahue, N.M., Prevot, A.S.H., Zhang, Q., Kroll, J.H.: Evolution of Organic
19 Aerosols in the Atmosphere. *Science*, 326(5959), 1252-1529 (2009) doi:10.1126/science.1180353

20 Keene, W.C., Pszenny, A.A., Galloway, J.N., Hawley, M.E., 1986. Sea-salt corrections and interpretation of
21 constituent ratios in marine precipitation. *Journal of Geophysical Research: Atmospheres* 91 (D6), 6647-
22 6658

23 Lourens, A.S.M., Beukes, J.P., Van Zyl, P.G., Fourie, G.D., Burger, J.W., Pienaar, J.J., Read, C.E., Jordaan, J.H.:
24 Spatial and Temporal assessment of Gaseous Pollutants in the Mpumalanga Highveld of South Africa. *S.*
25 *Afr. J. Sci.* 107(1/2), Art. #269, 8 pages (2011) doi:10.4102/sajs.v107i1/2.269

26 Lourens, A.S.M., Butler, T.M., Beukes, J.P., Van Zyl, P.G., Beirle, S., Wagner, T. Re-evaluating the NO₂ hotspot
27 over the South African Highveld. *S. Afr. J. Sci.* 108(9/10), Art. #1146, 6 pages (2012) doi:10.4102/sajs.
28 v108i11/12.1146

29 Lourens, A.S.M., Butler, T.M., Beukes, J.P., Van Zyl, P.G., Fourie, G.D. and Lawrence, M.G., Investigating
30 atmospheric photochemistry in the Johannesburg-Pretoria megacity using a box model, South African

1 Journal of Science, S. Afr. J. Sci. 112(1/2), Art. #2015-0169, 11 pages (2016) <http://dx.doi.org/10.17159/sajs.2016/2015-0169>

2

3 Mouli, P. C., Mohan, S. V., and Reddy, S. J.: A study on major inorganic ion composition of atmospheric aerosols

4 at Tirupati. *J Hazard Mater.* B96, 217–228 (2003)

5 Ng, N.L., Herndon, S.C., Trimborn, A., Canagaratna, M.R., Croteau, P.L., Onasch, T.B., Sueper, D., Worsnop,

6 D.R., Zhang, Q., Sun, Y.L., Jayne, J.T.: An Aerosol Chemical Speciation Monitor (ACSM) for Routine

7 Monitoring of the Composition and Mass Concentrations of Ambient Aerosol. *Aerosol Sci. Tech.* 45(7),

8 780-794 (2011) doi:10.1080/02786826.2011.560211

9 Pathak, R. K., Wang, T., Ho, K. F., and Lee, S. C.: Characteristics of summertime PM_{2.5} organic and elemental

10 carbon in four major Chinese cities: implications of high acidity for water-soluble organic carbon (WSOC).

11 *Atmos. Environ.* 45, 318–325 (2011) doi:10.1016/j.atmosenv.2010.10.021

12 Petäjä, T., Vakkari, V., Pohja, T., Nieminen, T., Laakso, H., Aalto, P.P., Keronen, P., Siivola, E., Kerminen, V.-

13 M., Kulmala, M., Laakso, L.: Transportable aerosol characterization trailer with trace gas chemistry:

14 design, instruments and verification. *Aerosol Air Qual. Res.* 13, 421–435 (2013)

15 Pope, C.A., Dockery, D.W. Health Effects of Fine Particulate Air Pollution: Lines that Connect. *Journal of the Air*

16 *& Waste Management Association.* 56(6), 709-742 (2006) doi.org/10.1080/10473289.2006.10464485

17 Pöschl, U. Atmospheric aerosols: composition, transformation, climate and health effects. *Angew. Chem. Int. Ed.*

18 44(46), 7520-7540 (2005) doi:10.1002/anie.200501122

19 Seinfeld, J.H., Pandis, S.N. *Atmospheric Chemistry and Physics.* New Jersey: John Wiley & Sons (2006)

20 Sinha, P., Lyatt, J., Hobbs, P.V., Liang, Q.: Transport of biomass burning emissions from southern Africa. *J.*

21 *Geophys. Res.: Atmospheres.* 109(D20), 8072 (2004) doi:10.1029/2004JD005044.

22 Stohl, A., Eckhardt, S., Forster, C., James, P., Spichtinger, N., Seibert, P.: A replacement for simple back trajectory

23 calculations in the interpretation of atmospheric trace substance measurements. *Atmos. Environ.* 36, 4635–

24 4648 (2002) [http://dx.doi.org/10.1016/S1352-2310\(02\)00416-8](http://dx.doi.org/10.1016/S1352-2310(02)00416-8)

25 Tiitta, P., Vakkari, V., Josipovic, M., Croteau, P., Beukes, J.P., Van Zyl, P.G., Venter, A.D., Jaars, K., Pienaar,

26 J.J., Ng, N.L., Canagaratna, M.R., Jayne, J.T., Kerminen, V.-M., Kulmala, M., Laaksonen, A., Worsnop,

27 D.R. Laakso, L.: Chemical composition, main sources and temporal variability of PM₁ aerosols in southern

28 African grassland. *Atmos. Chem. Phys.* 4, 1909–1927 (2014) doi:10.5194/acp-14-1909-2014

1 Turner, J. & Colbeck, I. Chapter 1: Physical and Chemical Properties of Atmospheric Aerosols, In: Colbeck, I.,
2 Editor, Environmental Chemistry of Aerosols, Volume 70, pp. 1–30, Blackwell Publishing Ltd, Oxford,
3 UK (2008) doi: 10.1002/9781444305388

4 Vakkari, V., Beukes, J.P., Laakso, H., Mabaso, D., Pienaar, J.J., Kulmala, M., Laakso, L.: Long-term observations
5 of aerosol size distributions in semi-clean and polluted savannah in South Africa. *Atmos. Chem. Phys.*
6 13(4), 1751-1770 (2013) doi:10.5194/acpd-12-24043-2012

7 Vakkari, V., Kerminen, V.-M., Beukes, J.P., Tiitta, P., Van Zyl, P.G., Josipovic, M., Venter, A.D., Jaars, K.,
8 Worsnop, D.R., Kulmala, M., Laakso, L.: Rapid changes in biomass burning aerosols by atmospheric
9 oxidation. *Geophys. Res. Lett.* 41, 2644–2651 (2014) doi:10.1002/2014GL059396

10 Vakkari, V., O’connor, E.J., Nisantzi, A., Mamouri, R.E., Hadjimitsis, D.G.: Low-level mixing height detection
11 in coastal locations with a scanning Doppler lidar. *Atmos. Meas. Tech.* 8(4), 1875-1885 (2015)
12 doi:10.5194/amt-8-1875-2015

13 Van Zyl, P.G., Beukes, J.P., Du Toit, G., Mabaso, D., Hendriks, J., Vakkari, V., Tiitta, P., Pienaar, J.J., Kulmala,
14 M., Laakso, L.: Assessment of atmospheric trace metals in the western Bushveld Igneous Complex, South
15 Africa. *S. Afr. J. Sci.* 110(3/4), Art. #2013-0280, 11 pages (2014)
16 <http://dx.doi.org/10.1590/sajs.2014/20130280>

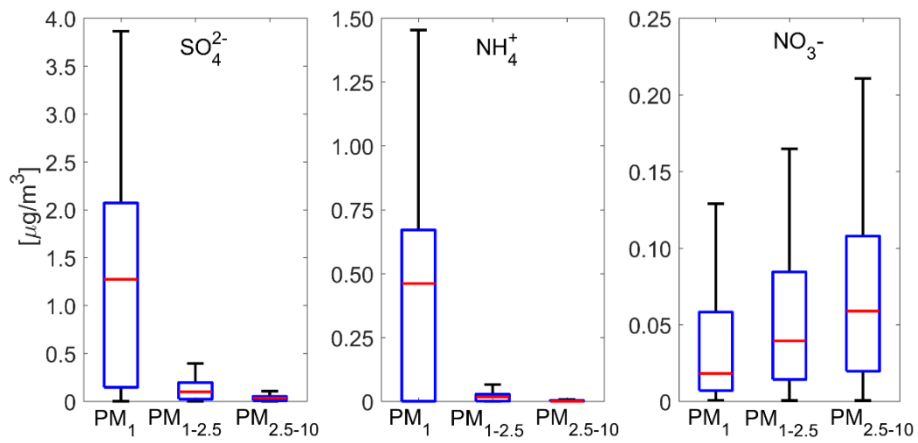
17 Venter, A. D., Vakkari, V., Beukes, J. P., Van Zyl, P. G., Laakso, H., Mabaso, D., Tiitta, P., Josipovic, M.,
18 Kulmala, M., Pienaar, J. J., Laakso, L.: An air quality assessment in the industrialised western Bushveld
19 Igneous Complex, South Africa. *S. Afr. J. Sci.* 108(9/10), Art. #1059, 10 pages (2012) doi: 10.4102/sajs.
20 v108i9/10.1059

21 Venter, A.D., Van Zyl, P.G., Beukes, J.P., Jaars, K., Josipovic, M., Booyens, W., Hendriks, J., Vakkari, V., Laakso,
22 L.: Measurement of atmospheric trace metals at a regional background site (Welgegund) in South Africa.
23 *Atmos. Chem. Phys.* 17, 4251–4263, (2017) doi:10.5194/acp-17-4251-2017

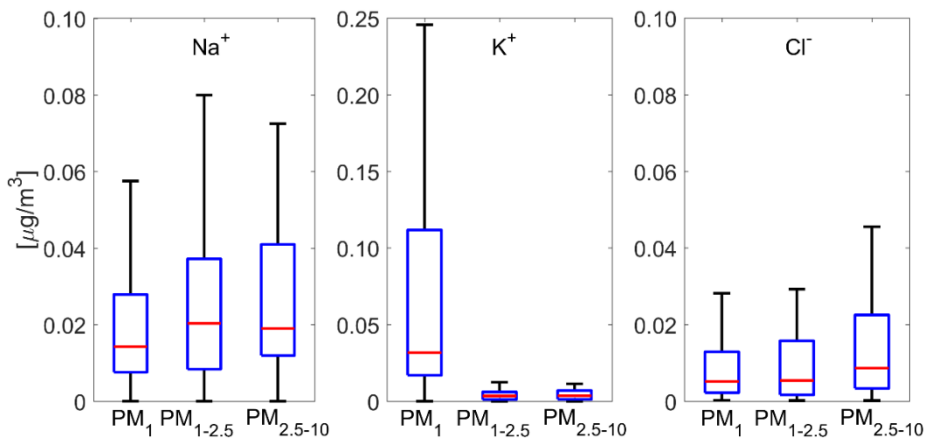
24 Wai, K.M., Wu, S., Kumar, A., Liao, H.: Seasonal variability and long-term evolution of tropospheric composition
25 in the tropics and Southern Hemisphere. *Atmos. Chem. Phys.* 14, 4859-4874 (2014) doi: 10.5194/acpd-13-
26 20011-2013

27 Xiao Z, Laplante AR.: Characterizing and recovering the platinum group minerals – a review. *Miner. Eng.* 17,
28 961–979 (2004) doi:10.1016/j.mineng.2004.04.001

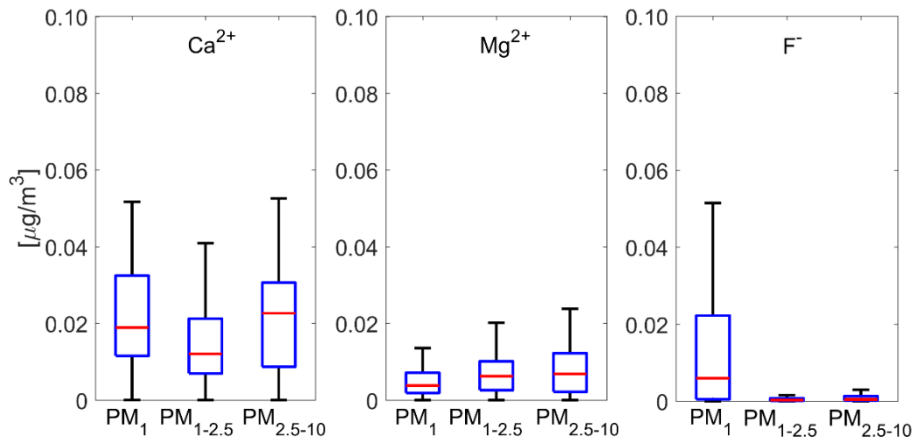
- 1 Yeh, S.-W., Park, R.J., Kim, M.J., Jeong, J.I., Song, C.-K.: Effect of anthropogenic sulphate aerosol in China on
2 the drought in the western-to-central US, *Nature: Scientific Reports*. 5, 14305 (2015) doi:
3 10.1038/srep14305
- 4 Zhang, Q.I., Jimenez, J.L., Worsnop, D.R., Canagaratna, M.: A case study of urban particle acidity and its influence
5 on secondary organic aerosol. *Environ. Sci. Tech.* 41(9), 3213-3219 (2007) doi:10.1021/es061812j



1



2

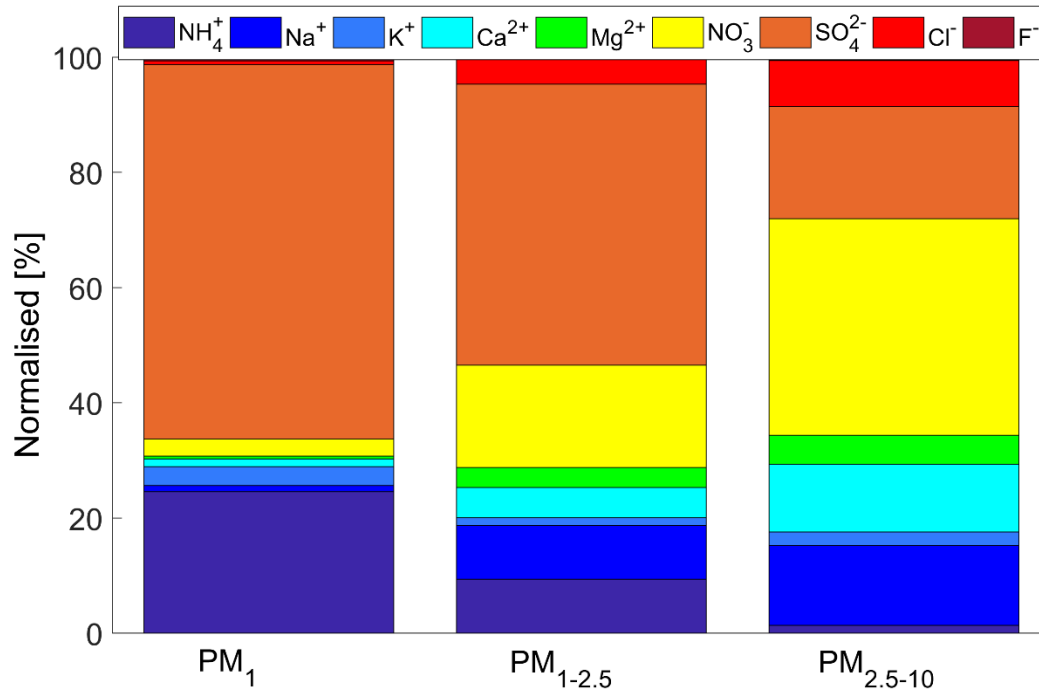


3

4 **Fig. 1** Boxplots of the concentrations of inorganic ionic species for PM_1 , $\text{PM}_{1-2.5}$ and $\text{PM}_{2.5-10}$ measured at
 5 Welgegend. The median (red line), 25th and 75th percentiles (blue box) and ± 2.7 times the standard deviation
 6 (whiskers) are indicated

7

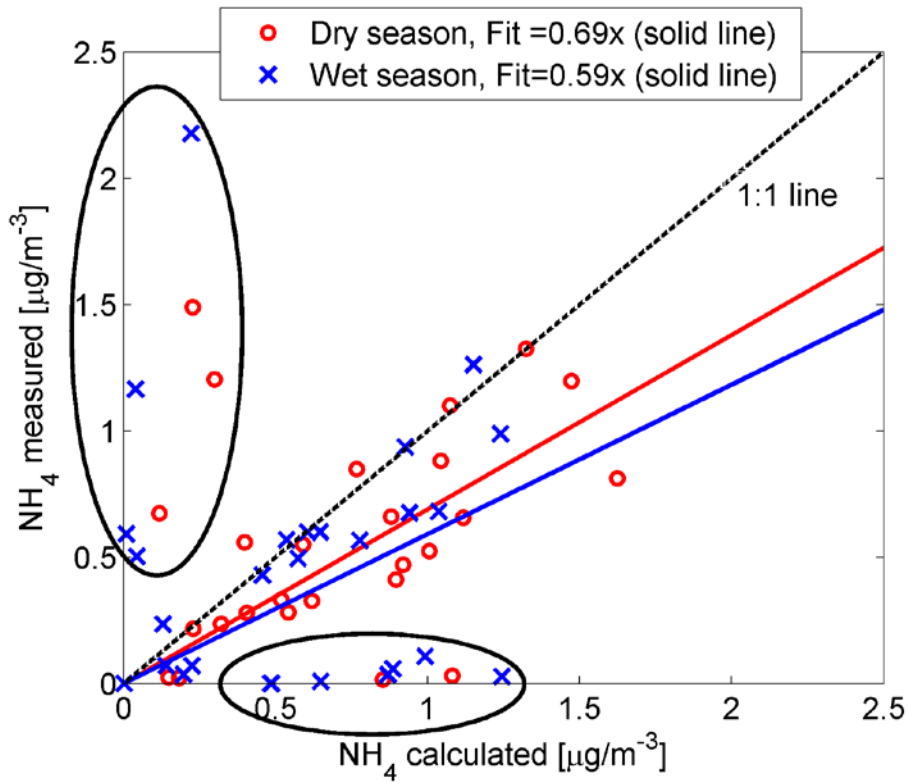
1



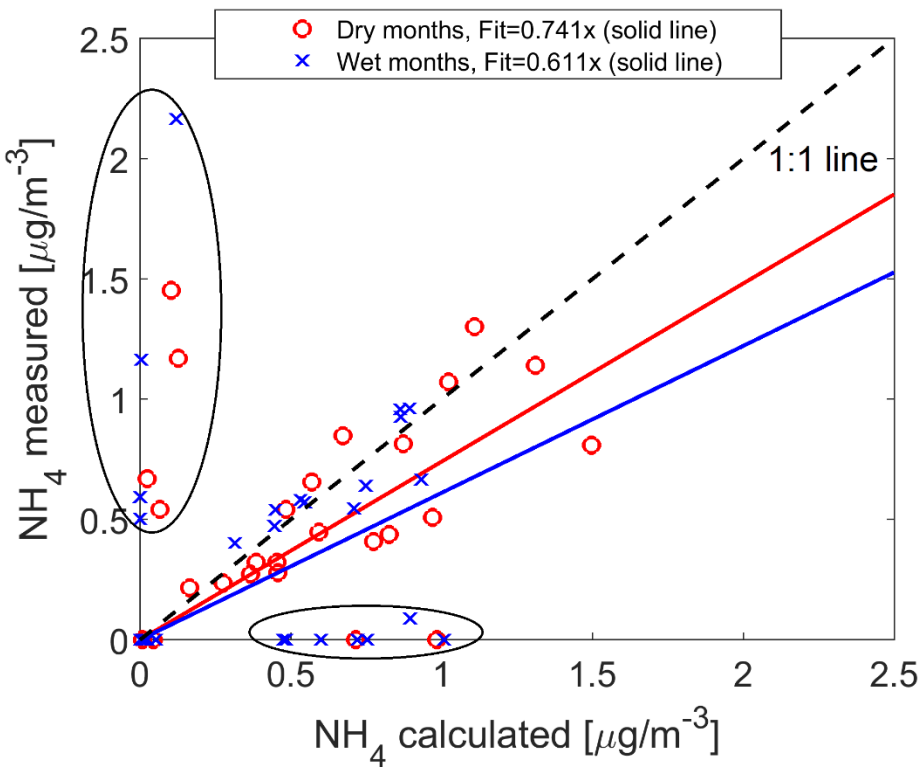
2

3 **Fig. 2** Normalised concentration distribution of the inorganic ionic species measured at Welgegund

4



1



2

3 **Fig. 3** The measured NH_4 concentrations are plotted in relation to the calculated NH_4 values for PM_{10} . The red
 4 circle and red trend line represent the dry months, while the blue crosses and blue trend line are for the wet months

5

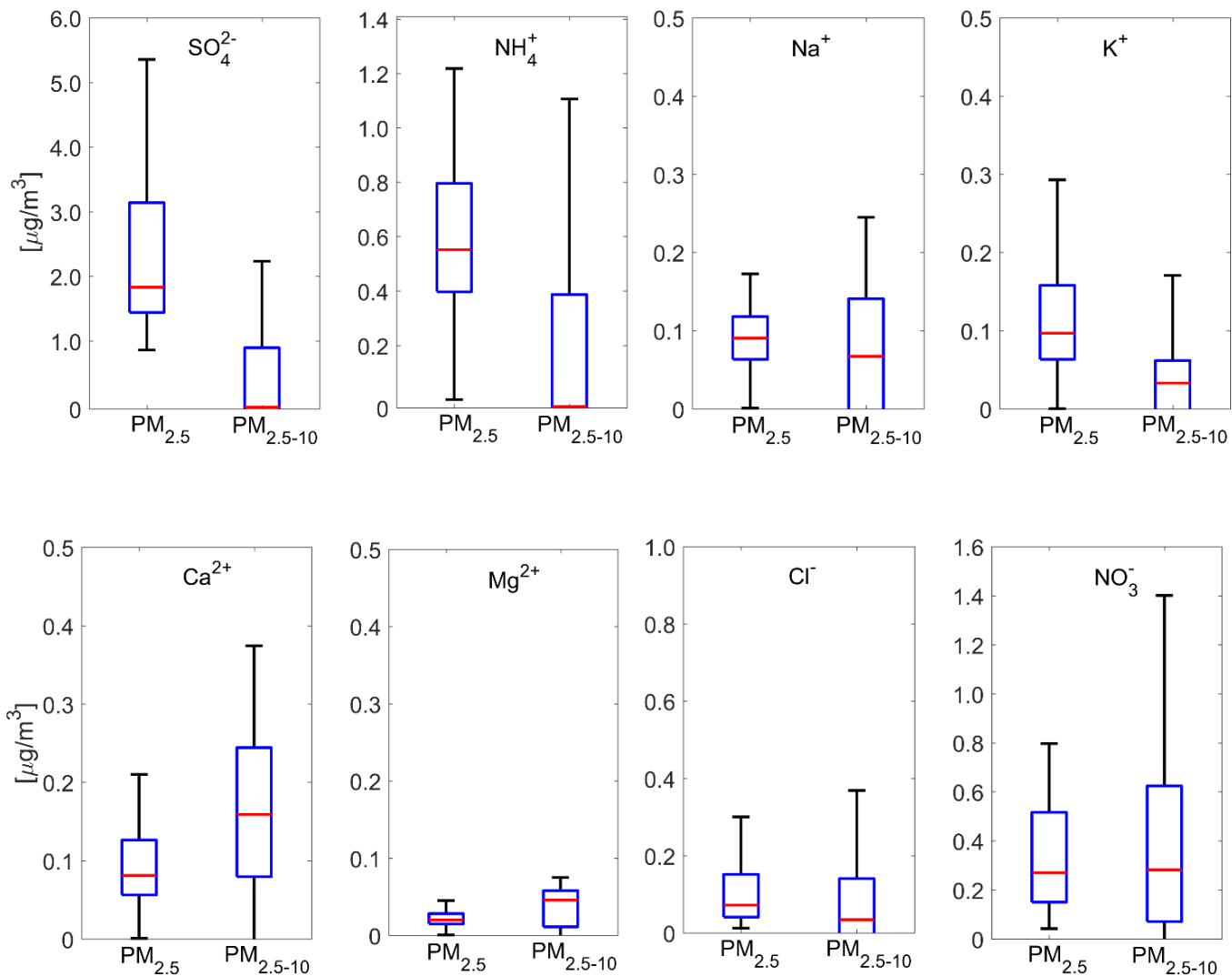
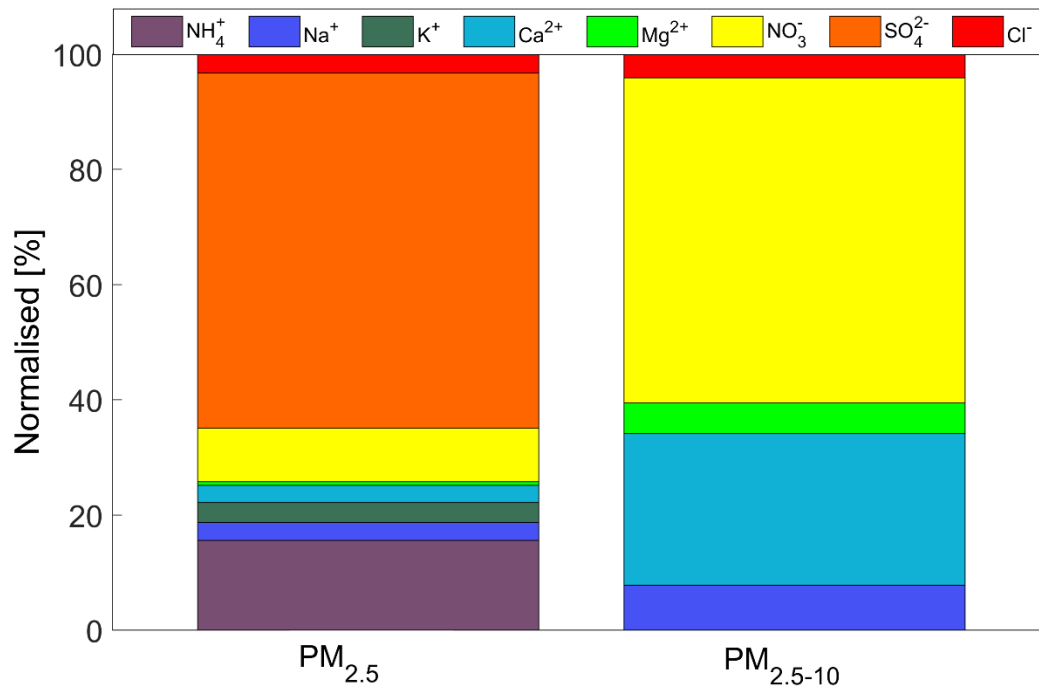


Fig. 4 Boxplots of the concentrations of inorganic ionic species for $\text{PM}_{2.5}$, and $\text{PM}_{2.5-10}$ measured at Marikana. The median (red line), 25th and 75th percentiles (blue box) and ± 2.7 times the standard deviation (whiskers) are indicated



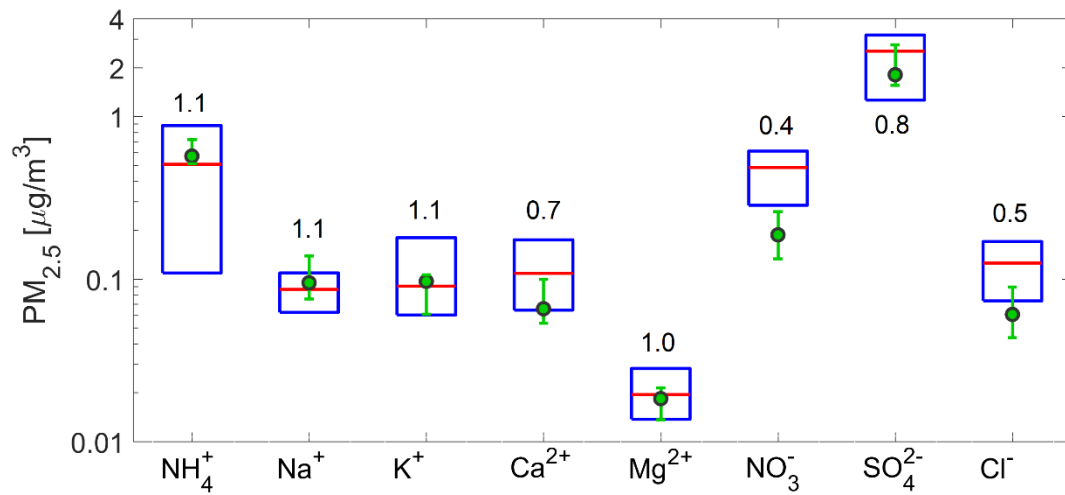
1

2

Fig. 5 Normalised concentration distribution of inorganic ionic species measured at Marikana

3

1

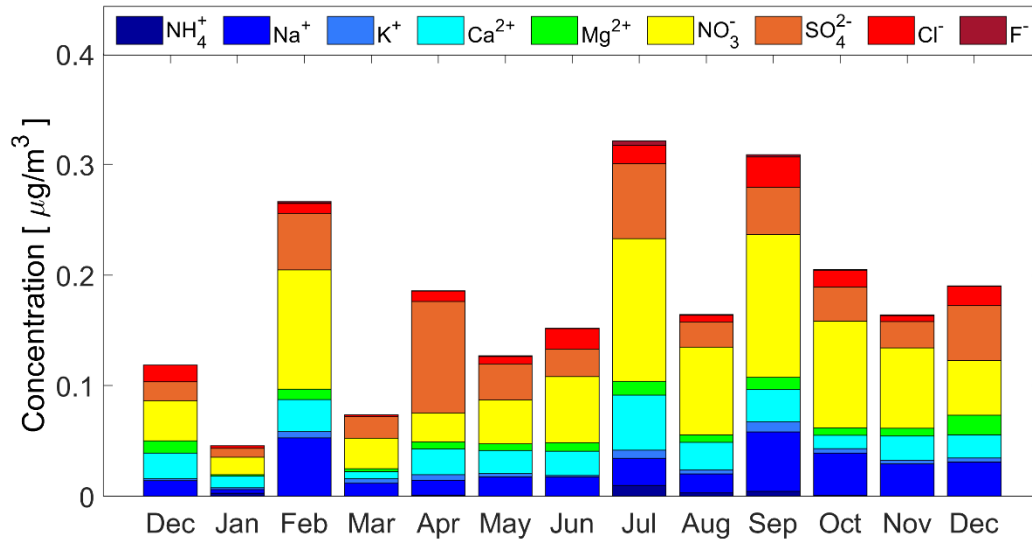


2

3 **Fig. 6** Concentrations of inorganic ionic species measured at Marikana during the daytime (circle) and night time
4 (box plots). For daytime measurements the green circle represent the median values and the green whiskers the
5 25th and 75th percentiles, while for night-time measurements the red line represent the median and the blue box
6 the 25th and 75th percentiles

7

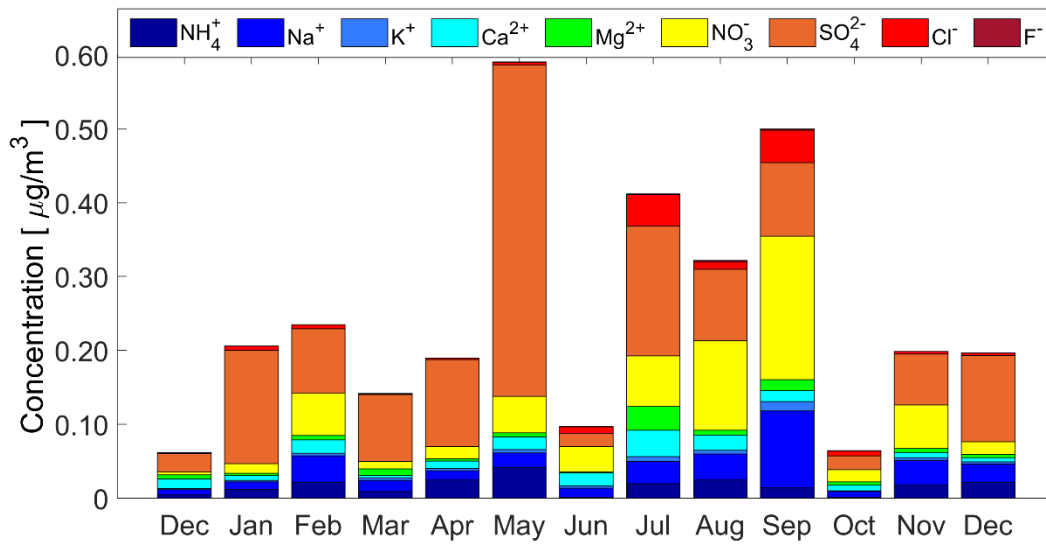
1



2

3

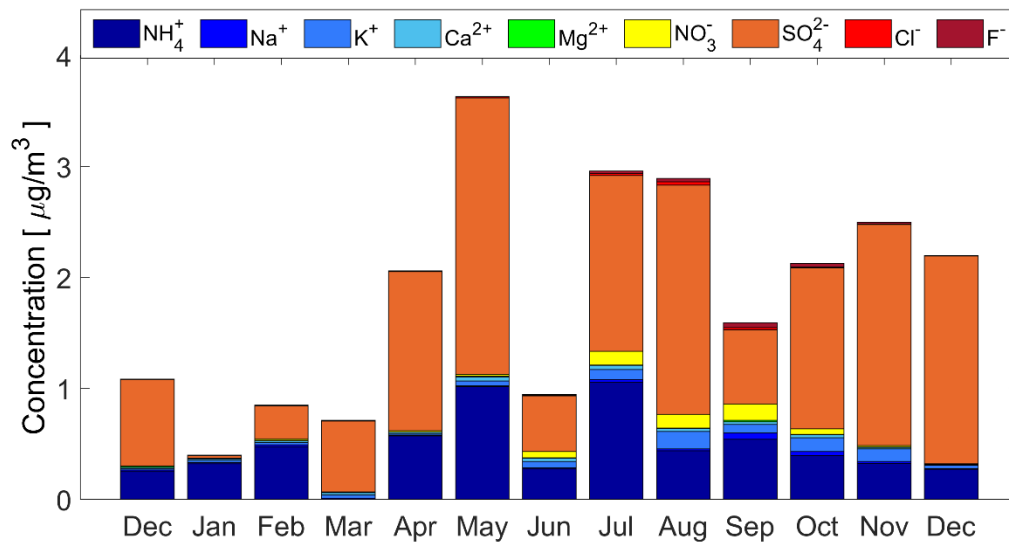
(a)



4

5

(b)

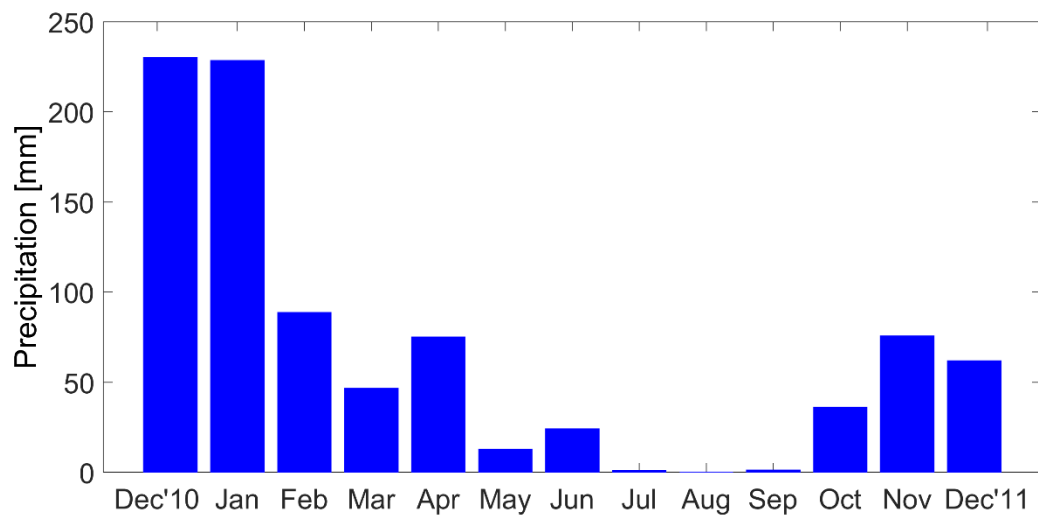


1
2
3
4

(c)

Fig. 7 Welgegend monthly median inorganic ion concentrations for (a) PM_{2.5-10}, (b), PM_{1-2.5} and (c), PM₁

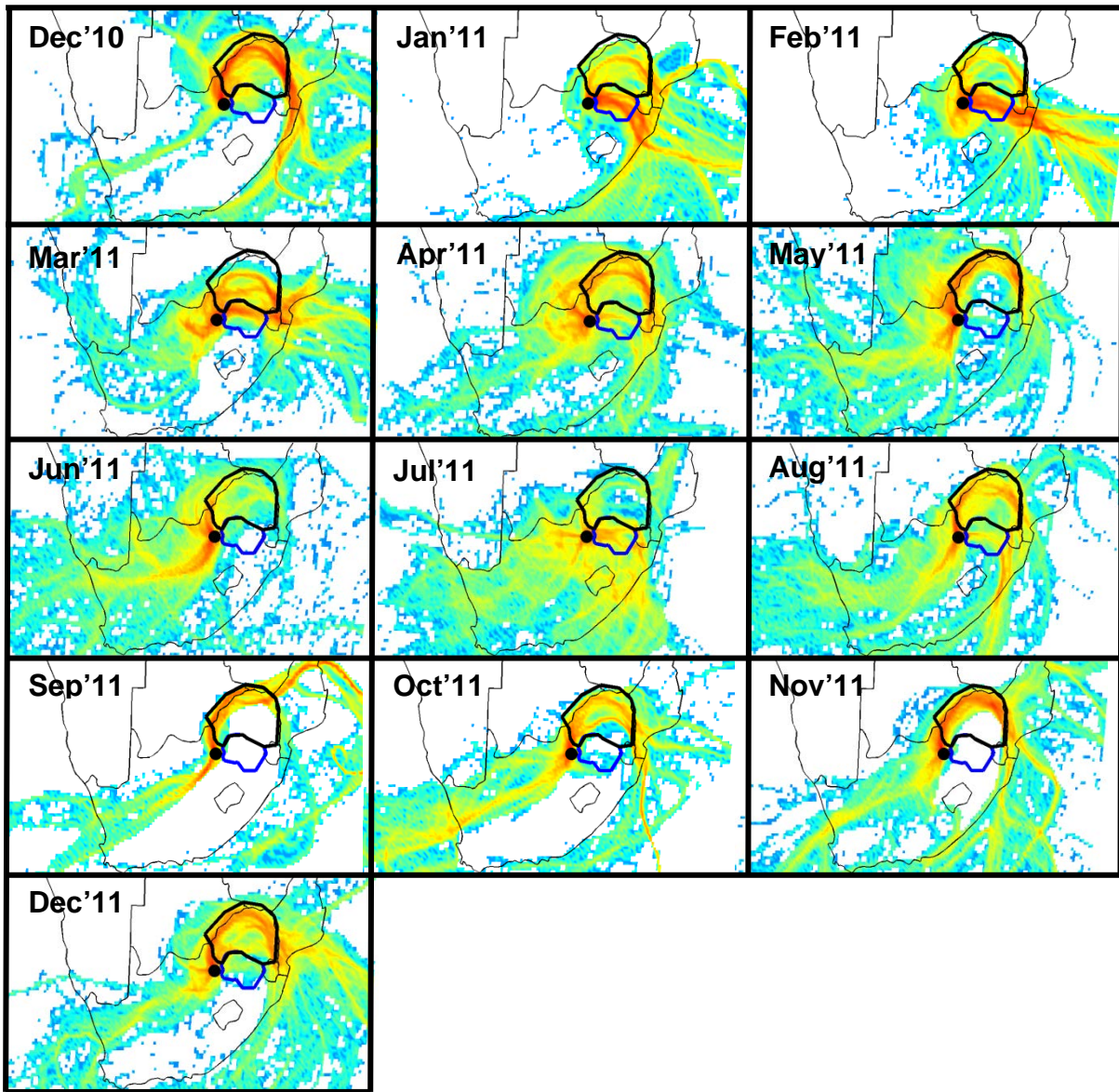
1



2

3 **Fig. 8** Monthly accumulated rainfall measured at Welgegund for the sampling duration

4



1
 2 **Fig. 9** Monthly air-mass back trajectories as measured at Welgegund (black dot) during the sampling period. The
 3 colour scale indicates the percentage of trajectories passing over $0.2^\circ \times 0.2^\circ$ grid cells, with blue to yellow to red
 4 indicating the lowest to highest frequency of air mass movement. The black polygon in the northern parts of South
 5 Africa indicates the typical anticyclonic recirculation area while the blue polygon contains the location of the
 6 majority of South African industries

7

1 **Table 1** Ratios of species to Na⁺ in PM and reference seawater ratios (Keene et al., 1986)

	SO ₄ ²⁻ /Na ⁺	Cl ⁻ /Na ⁺	K ⁺ /Na ⁺	Mg ²⁺ /Na ⁺	Ca ²⁺ /Na ⁺
Sea water	0.121	1.161	0.022	0.227	0.044
PM ₁	67.02	0.48	2.46	0.24	1.38
PM _{1-2.5}	3.51	0.34	0.17	0.27	0.72
PM _{2.5-10}	1.28	0.57	0.16	0.29	0.92

2